https://doi.org/10.2298/SOS220802023M

Submitted: 02.08.2022.
Accepted for publication: 28.10.2022.
UDK: 666.3.019; 622.785

Synthesis and Characterization of High-Entropy $A_2B_2O_7$ Pyrochlore with Multiple Elements at A and B Sites

Branko Matović[1,4,*], Jelena Maletaškić[1], Vesna Maksimović[1], Silvana Dimitrijević[2], Bratislav Todorović[3], Jelena Zagorac[1], Aleksa Luković[1], Yu-Ping Zeng[4], Ivana Cvijović-Alagić[1]

[1]Center of Excellence "CEXTREME LAB", Vinča Institute of Nuclear Sciences - National Institute of the Republic of Serbia, University of Belgrade, Mike Petrovića Alasa 12-14, 11001 Belgrade, Serbia

[2] Mining and Metallurgy Institute Bor, Zeleni Bulevar 35, 19210 Bor, Serbia

[3]Faculty of Technology Leskovac, University of Niš, Bulevar Oslobođenja 124, 16000 Leskovac, Serbia

[4]State Key Laboratory of High Performance Ceramics and Superfine Microstructure, Shanghai Institute of Ceramics, Chinese Academy of Sciences, 1295 Ding-xi Road, Shanghai 200050, China

Corresponding author: mato@vin.bg.ac.rs

Abstract

Single nano high-entropy pyrochlore-type compound ($A_2B_2O_7$) with 7 different rare-earth cations at site A and 3 different metal cations at site B with equiatomic amounts $(7A_{1/7})_2(3B_{1/3})_2O_7$ is successfully obtained. The powder with nominal composition $(La_{1/7}Sm_{1/7}Nd_{1/7}Pr_{1/7}Y_{1/7}Gd_{1/7}Yb_{1/7})_2(Sn_{1/3}Hf_{1/3}Zr_{1/3})_2O_7$ was fabricated by reacting metal nitrates (site A) and metal chlorides (site B) with glycine during the combustion reaction. The XRD analysis revealed that the powder attained during synthesis is in an amorphous state. To induce crystallization of the obtained pyrochlore

structure, the post-calcination process at 600-1500 °C was conducted and studied. Results of this study showed that the monophase pyrochlore ($A_2B_2O_7$) structure is obtained during the calcination at 900 °C. The high-density ceramic pellet with 97% of theoretical density and free of any additives was obtained through pressureless sintering at 1650 °C for 4 h in the air using the powder calcined at 900 °C.

Keywords: High-entropy pyrochlore; Combustion reaction; Monophase structure; High-density ceramic

1. Introduction

Complex compounds with the general chemical formula $A_2B_2O_7$ are known as pyrochlores since being isostructural to mineral pyrochlore $NaCa(Nb,Ta)_2O_6$-(OH/F) [1]. Recently, high-entropy pyrochlores gained significant attention from the scientific community due to the interesting combination of their new or improved properties compared to normal pyrochlores, such as better phase stability and chemical resistance, increased melting points, lower thermal conductivity, and excellent resistance to radiation-induced amorphization [2-6].

In a pyrochlore-type formula, the letter A denotes the site occupied by a larger trivalent 8-coordinated cation, typically a rare-earth (RE) element, whereas B represents a smaller tetravalent 6-coordinated cation of transition metal (Me), such as Ti, Zr, and Hf [7]. The compound can exist in two closely related structures known as the ordered pyrochlore structure (space group 227) and the disordered fluorite structure (space group 225) [8].

The properties and crystal structure of pyrochlores are highly dependent on their composition and the ratio of radii of A-site cation (rA^{3+}) and B-site cation (rB^{4+}). Normally the pyrochlore-type structure is observed for radius ratio rA^{3+}/rB^{4+} = 1.46-1.78, especially when one site can be occupied by several potential elements [7].

Many different approaches were used over the years for the synthesis of pyrochlore ceramics, such as the solid-state reaction method [9], precipitation and combustion synthesis [10], hydrothermal route [11], sol-gel method [12], mechanical grinding [13], solid-state displacement reaction at low temperature [14], and molten salt reaction [15]. Since combustion synthesis was successfully used for the synthesis of a

significant number of different oxide compounds and their solid solutions, it can be assumed that this approach could be effectively applied to the synthesis of multicomponent oxides, such as high-entropy pyrochlores [16,17].

The goal of this research, therefore, was to obtain a chemically complex multicomponent oxide with the $A_2B_2O_7$ pyrochlore structure that contains 10 different cations in equiatomic amounts using the combustion reaction. This approach to the synthesis was chosen because it provides excellent mixing of the constituent elements at the atomic level, enabling the formation of the desired compound composition at a relatively low temperature. Phase development during the calcination process, sinterability of the obtained powder, as well as some properties of the sintered high-entropy multicomponent oxide were investigated.

2. Materials and Experimental Procedures

2.1. Material synthesis

The precursors used for the synthesis of the high-entropy complex oxide with a pyrochlore structure were 99.9% pure RE nitrates in the form of hexahydrate (RE = La, Nd, Yb, Nd, Gd, Sm, Y), and Me chlorides (Me = Zr, Hf, Sn) supplied by Sigma-Aldrich, USA, as well as 98.5% pure glycine supplied by the same company as fuel.

All initial reactants were dissolved in distilled water and added according to the previously calculated composition of the final powder. The reaction took place in a stainless steel reactor according to the following equation:

$$2Me^{III}(NO_3)_3\cdot 6H_2O+2Me^{IV}Cl_4+4NH_2CH_2COOH+3O_2 =$$

$$(La_{1/7}Sm_{1/7}Nd_{1/7}Pr_{1/7}Y_{1/7}Gd_{1/7}Yb_{1/7})_2(Sn_{1/3}Hf_{1/3}Zr_{1/3})_2O_7+5N_2+8CO_2+18H_2O+8HCl \quad (1)$$

(39 mol of gases/mol of $(La_{1/7}Sm_{1/7}Nd_{1/7}Pr_{1/7}Y_{1/7}Gd_{1/7}Yb_{1/7})_2(Sn_{1/3}Hf_{1/3}Zr_{1/3})_2O_7$)

where Me^{III} represents La, Nd, Yb, Nd, Gd, Sm, Y, while Me^{IV} denotes Zr, Hf, and Sn. It should be underlined that the reaction presented in Eq.(1) is a complex multi-stage process, which is explained in detail elsewhere [18] and which is here presented in its simplified final form.

A clear solution of all metal salts mixture was heated in the reactor, where the reaction after ignition proceeds spontaneously and terminates extremely fast at approximately 450 °C with the strong release of gaseous products, which is in good agreement with Eq.(1). The resulting ash powder was calcined to burn the organic components and obtain a pure homogeneous oxide powder with the desired stoichiometry. Calcination was carried out in the temperature range from 600 °C to 1500 °C with a holding time of 2 h at each target temperature. The produced powders were uniaxial compressed without the use of binders at 200 MPa into discs with a diameter of 16 mm and thickness of 5 mm. The green pellets were pressureless sintered in a laboratory furnace at 1650 °C with a heating rate of 10 °C/min and a soaking time of 4 h.

2.2. Materials characterization

The X-ray diffractometer (XRD) RIGAKU Ultima IV, Rigaku Corporation, Japan, with Ni-filtered Cu Kα radiation (λ = 1.54178 Å) was used for phase analysis of calcined powders and sintered pellets. The XRD measurements were performed in the 2θ range from 10° to 90°. Identification of the present phases was conducted using the PDXL2 *v*. 2.0.3.0 software, with reference to the International Center for Diffraction Data (ICDD) patterns *v*. 2012 [19], using the ICDD card No. 00-013-0183.

The Rietveld structural refinement calculations were conducted using the obtained XRD data and the FullProf software to determine relevant structural parameters of the powders calcined at different temperatures. As initial structural parameters for the conducted Rietveld refinement calculations the ICSD database data for the $La_2Zr_2O_7$ compound (No. 26851) were utilized including the space group, unit cell parameters, and atomic positions information.

The Fourier-transform infrared spectroscopic (FT-IR) analysis was performed on the calcined and sintered samples to determine their chemical bonding and structure. The FT-IR measurements were performed at room temperature in the range of 4000-400 cm^{-1} with a resolution of 2 cm^{-1} using a Bomem MB-100 spectrometer, Hartmann & Braun, Canada, to obtain sub-formed spectra.

Morphology and elemental distribution of the obtained calcined powders and sintered ceramic samples were analyzed using a scanning electron microscope (SEM)

JSM-IT300LV, JEOL, Japan, operated at 20 keV and coupled with an X-max energy dispersive spectrometer (EDS), Oxford Instruments, UK.

The sintered sample microhardness was determined using a Buehler Micromet 5101Vickers indentation hardness tester, Buehler, Germany, by applying 1 kgf (9807 mN) of load for 15 s. Microhardness was evaluated at 12 measuring points and excellent reproducibility was demonstrated.

3. Results and Discussion

The typical morphology of the obtained compositionally complex oxide powder is shown in Fig. 1. The powder calcined at 600 °C depicted very small isometric particles which are heavily agglomerated to form bigger grains. The corresponding EDS mapping demonstrates that all cations were present in the analyzed powder sample according to its nominal composition. Moreover, the observed elemental distribution showed that elements were randomly and homogeneously distributed throughout the analyzed powder sample indicating that the powder chemical homogeneity was achieved as a result of the selected synthesis procedure.

Fig. 1

The XRD patterns presented in Fig. 2 indicate that the powder calcined at 600 °C shows typical amorphous behavior without a long range of atom ordering. On the other hand, powder calcined at 900 °C exhibits clearly visible reflections of pure crystalline pyrochlore phase in space group 227 ($Fd\bar{3}m$). Nevertheless, very broad diffraction lines in its XRD pattern indicate its low crystallinity state. The XRD analysis also showed that a further increase in the annealing temperature causes a narrowing of the diffraction lines and increasing in their intensities, which is a result of increased crystallite size.

Fig. 2

The XRD pattern recorded for the powder calcined at the highest temperature is therefore selected for further analysis by employing Rietveld's method. The result of the Rietveld structural refinement of the XRD pattern obtained for the powder calcined at 1500 ºC is presented in Fig. 3.

Fig. 3

The Rietveld method is also applied to attain cell parameters, crystallite size, and lattice strain parameters of the obtained powder calcined at different temperatures and attained data are given in Table I. Results of the refinement presented in Table I clearly show that the average crystallite size increases with an increase in the calcination temperature, while at the same time the internal strain decreases with an increase in the annealing temperature indicating the presence of the crystal growth process and the atomic arrangement ordering during the calcination. The reliability of the applied method was evaluated by determining R factors that indicate the goodness of fit (R_B). Low R_B values of 2.33, 1.76, and 4.77 attained for the samples calcined at 900 ºC, 1200 ºC, and 1500 ºC, respectively, showed that the conducted Rietveld refinement was successful.

Tab. I

The oxygen vacancy defect is extremely important when the crystal structure of pyrochlore is concerned (parameter *x* in Table I). The *x* position, *i.e. x* coordinate of O_1, can be in the range from 0.3125 (for ideal crystal structure) to 0.375 (for defect fluorite structure) [1]. In the present study, the *x* parameter of the obtained compositionally complex pyrochlore was determined to be between 0.320 and 0.336, depending on the calcination temperature, indicating that the obtained calcined materials show a highly ordered pyrochlore structure.

The FT-IR spectra of the obtained calcined powders were recorded at room temperature (Fig. 4). All analyzed samples depicted hygroscopicity despite their different calcination temperatures. The broad band observed in the wavenumber region of 3600-3200 cm^{-1} represents the stretching vibration of the O-H bond in water. Moreover, the peak present at 1635 cm^{-1} can be ascribed to a bending mode of water. The recorded spectra also indicate that the intensity of the O-H band decreases with an increase in the calcination temperature due to a decrease in the total surface area and increased atomic arrangement manifested by a decrease in hygroscopicity. The results of the FT-IR spectroscopic analysis are in good agreement with the XRD findings. The characteristic stretching vibrations of the metal-oxygen (M-O) bonds, present between numerous cations and oxygen, are identified in the 600-400 cm^{-1} region [20].

Fig. 4

SEM micrographs reveal that the synthesized multicomponent pyrochlore powder shows good sinterability. The resulting density of the sample sintered at 1650 °C was 97% of the theoretical density, indicating a relatively easy densification process during sintering at 1650 °C for 4 h without the use of sintering additives. The microstructure of the sintered pellet is shown in Fig. 5a. The attained microstructure consists of densely compacted isometric grains with a bimodal structure which is mainly composed of grains with dimensions ranging from 5 μm to 10 μm, revealing the tendency of calcined powders to coarsen during the sintering process. Moreover, all crystalline pyrochlore grains are in direct mutual contact without the presence of an amorphous or secondary phase at the grain boundaries and at the grain contact sites (Fig. 5b). This kind of microstructure shows significant advantages when the mechanical properties of ceramics are concerned, especially at elevated temperatures.

Fig. 5

Results of the combined SEM and EDS analysis of the sintered ceramic material indicate that all elements corresponding to its nominal composition are evenly and homogeneously distributed throughout the entire ceramic sample showing that good compositional uniformity was achieved (Fig. 5).

Due to the high density and low porosity of the samples attained during the sintering process, these samples are also characterized by a relatively high hardness of 8.3 GPa. Achieved hardness is considered to be mechanically sufficient for the usage of these materials as thermal barrier coatings.

4. Conclusion

A study on the synthesis and properties of multicomponent solid solutions with pyrochlore structure (high-entropy pyrochlore ceramic) was presented. The powders with nominal composition $(La_{1/7}Sm_{1/7}Nd_{1/7}Pr_{1/7}Y_{1/7}Gd_{1/7}Yb_{1/7})_2(Sn_{1/3}Hf_{1/3}Zr_{1/3})_2O_7$ were synthesized using the combustion reaction between metal hydrates, metal chlorides and glycine as fuel. Pure crystalline high-entropy pyrochlore powder was obtained by heat treatment at 900 °C. Densification of the green compacts was conducted without the usage of sintering aids by applying the pressureless sintering at 1650 °C for 4 h. The

microstructure of the obtained sintered high-entropy pyrochlore ceramic shows a bimodal structure with equiaxed grains, ranging from 5 μm to 10 μm in size. The EDS elemental mapping of the sintered ceramic shows that all elements present in its nominal composition are distributed randomly and homogeneously throughout the sample confirming its good compositional uniformity, which is in good agreement with the results of Rietveld refinement of the recorded XRD pattern. A relative density of 97%, as well as a microhardness value of 8.3 GPa were achieved indicating good mechanical properties and applicability of the obtained high-entropy pyrochlore ceramic.

Acknowledgments

This research was financially supported by the Ministry of Education, Science and Technological Development of the Republic of Serbia (Grant No. 451-03-68/2022-14/200017) and the Visiting Professor Program of the Chinese Academy of Sciences (2021VEA0003).

5. References

1. M.A. Subramanian, G. Aravamudan, G.V. Subba Rao, Prog. Solid. State. Ch., 15 (1983) 55-143.

2. D.R. Clarke, C.G. Levi, Annu. Rev. Mater. Res., 33 (2003) 383-417.

3. A.A. Gusev, I.P. Raevski, E.G. Avvakumov, V.P. Isupov, Sci. Sinter., 48(3) (2016) 283-292.

4. J. Díaz-Guillén, M. Díaz-Guillén, K. Padmasree A.F. Fuentes, J. Santamaría, C. León, Solid State Ion., 179 (2008) 2160-2164.

5. Ren K, Wang Q, Shao G, X. Zhao, Y. Wang, Scripta Mater., 178 (2020) 382-386.

6. V.D. Risovany, A.V. Zakharov, E.M. Muraleva, V.M. Kosenkov, R.N. Latypov, J. Nucl. Mater., 355 (2006) 163-170.

7. A.F. Fuentes, S.M. Montemayor, M. Maczka, M. Lang, R.C. Ewing, U. Amador, Inorg. Chem., 57 (2018) 12093-12105.

8. Rost CM, Sachet E, Borman T, A. Moballegh, E.C. Dickey, D. Hou, J.L. Jones, S. Curtarolo, J-P. Maria, Nat. Commun., 6 (2015) 8485.

9. Z. Wang, G. Zhou, X. Qin, F. Zhang, J. Ai, P. Liu, S. Wang, J. Eur. Ceram. Soc., 34 (2014) 3951-3958.

10. T. Jeyasingh, S. Saji, P. Wariar, AIP Conference Proceedings, 1859 (2017) 020016.

11. J. Zeng, H. Wang, Y. Zhang, M.K. Zhu, H. Yan, J. Phys. Chem. C, 111 (2007) 11879-11887.

12. S. Wang, W. Li, S. Wang, Z. Chen, J. Eur. Ceram. Soc., 35 (2015) 105-112.

13. A.F. Fuentes, K. Boulahya, M. Maczka, J. Hanuza, U. Amador, Solid State Sci., 7 (2005) 343-353.

14. B. Matovic, J. Maletaskic, D. Bucevac, J. Zagorac, M. Fajar, K. Yoshida, T. Yano, Ceram. Int., 44 (2018) 16972-16976.

15. M.L. Hand, M.C. Stennett, N.C. Hyatt, J. Eur. Ceram. Soc., 32 (2012) 3211-3219.

16. B. Matović, D. Zagorac, I. Cvijović-Alagić, J. Zagorac, S. Butulija, J. Erčić, O. Hanzel, R. Sedlák, M. Lisnichuk, P. Tatarko, Bol. Soc. Esp. Ceram. Vidr., https://doi.org/10.1016/j.bsecv.2021.11.002

17. K. Zhang, W. Li, J. Zeng, T. Deng, B. Luo, H. Zhang, X. Huang, J. Alloys Compound., 817 (2020) 153328.

18. B. Matovic, J. Maletaskic, J. Zagorac, V. Pavkov, R.S. Maki, K. Yoshida, T. Yano, J. Eur. Ceram. Soc., 40 (2020) 2652-2657.

19. PDXL2 Version 2.0.3.0 Integrated X-ray Powder Diffraction Software, Rigaku Corporation, Tokyo, Japan, (2011) 196-8666.

20. G. Korotcenkov, S.D. Han, B. Cho, V. Tolstoy, Process. Appl. Ceram., 3 (2009) 19-28.

Сажетак

Наночестично високоентропијско пирохлорно једињење ($A_2B_2O_7$) са 7 различитих катјона ретких земаља на сајту А и 3 различита метална катјона на сајту В са једнаким бројем атома ($(7A_{1/7})_2(3B_{1/3})_2O_7$) је успешно синтетисано. Прах номиналног састава $(La_{1/7}Sm_{1/7}Nd_{1/7}Pr_{1/7}Y_{1/7}Gd_{1/7}Yb_{1/7})_2(Sn_{1/3}Hf_{1/3}Zr_{1/3})_2O_7$ је добијен реакцијом металних нитрида (сајт А) и металних хлорида (сајт В) са глицином током реакције сагоревања. Рендгенска дифракциона анализа је показала да је синтетисани прах аморфан. Како би се иницирала кристализација у пирохлорну структуру, прах је подвргнут накнадној калцинацији на температурама у распону од 600 °C до 1500 °C и детаљно испитан. Резултати испитивања су показали да је монофазна пирохлорна ($A_2B_2O_7$) структура образована током процеса калцинације на температури од 900 °C. Изразито густи керамички материјал без присуства адитива и са 97% теоријске густине је са успехом образован процесом синтеровања на 1650 °C у трајању од 4 сата на ваздуху без примене притиска коришћењем праха калцинисаног на 900 °C.

Кључне речи: високоентропијски пирохлор; реакција сагоревања; монофазна структура; густа керамика

Figure Captions

Fig. 1. SEM micrograph with corresponding EDS mapping of the synthesized $(La_{1/7}Sm_{1/7}Nd_{1/7}Pr_{1/7}Y_{1/7}Gd_{1/7}Yb_{1/7})_2(Sn_{1/3}Hf_{1/3}Zr_{1/3})_2O_7$ pyrochlore compound calcined at 600 °C for 2 h.

Fig. 2. Calcined $(La_{1/7}Sm_{1/7}Nd_{1/7}Pr_{1/7}Y_{1/7}Gd_{1/7}Yb_{1/7})_2(Sn_{1/3}Hf_{1/3}Zr_{1/3})_2O_7$ powders treated for 2 h at different temperatures: a) 600 °C, b) 900 °C, c) 1200 °C, and d) 1500 °C.

Fig. 3. Rietveld refinement of the XRD pattern obtained for the sample calcined at 1500 ^oC.

Fig. 4. FT-IR spectra of the powders calcined at different temperatures: a) 900 °C, b) 1200 °C, c) 1500 °C.

Fig. 5. a),c) SEM micrographs with c),d) corresponding EDS elemental maps of the pyrochlore compound $(La_{1/7}Sm_{1/7}Nd_{1/7}Pr_{1/7}Y_{1/7}Gd_{1/7}Yb_{1/7})_2(Sn_{1/3}Hf_{1/3}Zr_{1/3})_2O_7$ sintered at 1650 °C for 4 h showing a) grains morphology, b) grains contact, c) distribution of B-site elements, d) distribution of A-site elements and oxygen.

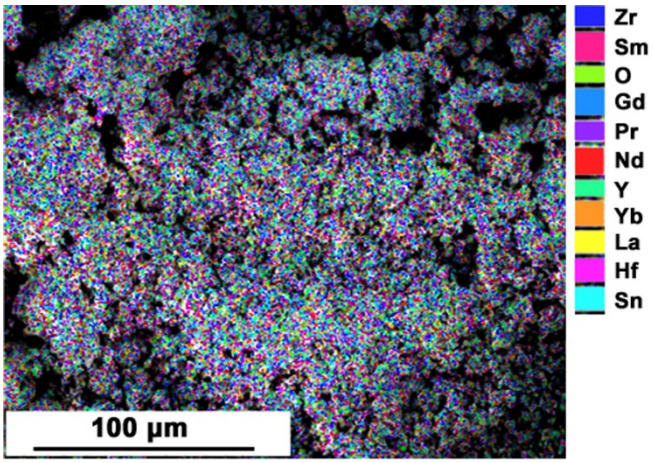

Fig. 1. SEM micrograph with corresponding EDS mapping of the synthesized $(La_{1/7}Sm_{1/7}Nd_{1/7}Pr_{1/7}Y_{1/7}Gd_{1/7}Yb_{1/7})_2(Sn_{1/3}Hf_{1/3}Zr_{1/3})_2O_7$ pyrochlore compound calcined at 600 °C for 2 h.

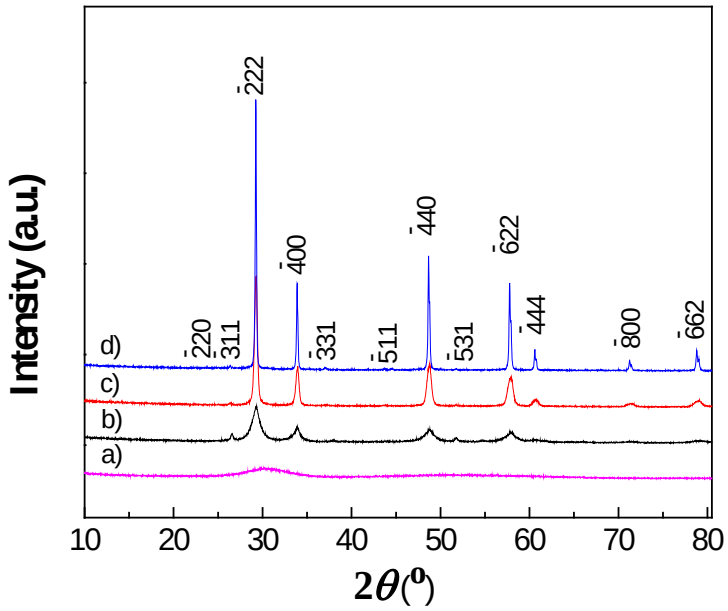

Fig. 2. Calcined $(La_{1/7}Sm_{1/7}Nd_{1/7}Pr_{1/7}Y_{1/7}Gd_{1/7}Yb_{1/7})_2(Sn_{1/3}Hf_{1/3}Zr_{1/3})_2O_7$ powders treated for 2 h at different temperatures: a) 600 °C, b) 900 °C, c) 1200 °C, and d) 1500 °C.

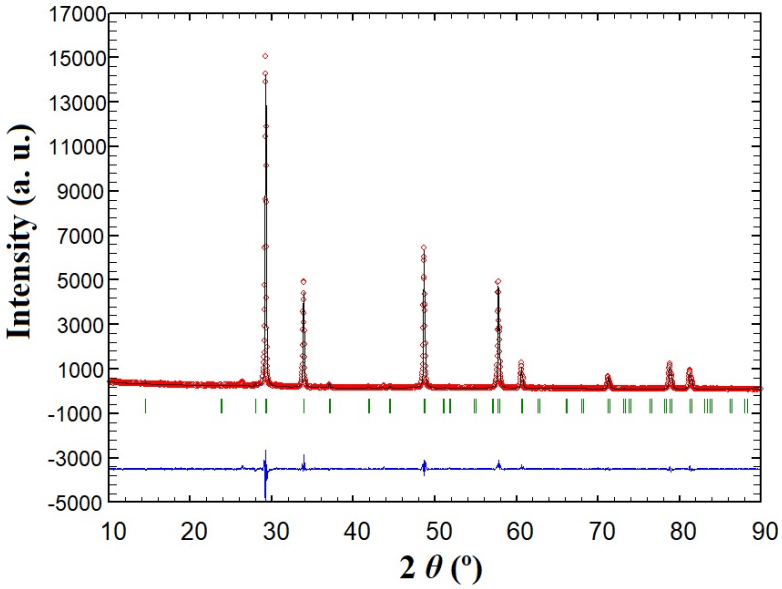

Fig. 3. Rietveld refinement of the XRD pattern obtained for the sample calcined at 1500 ºC.

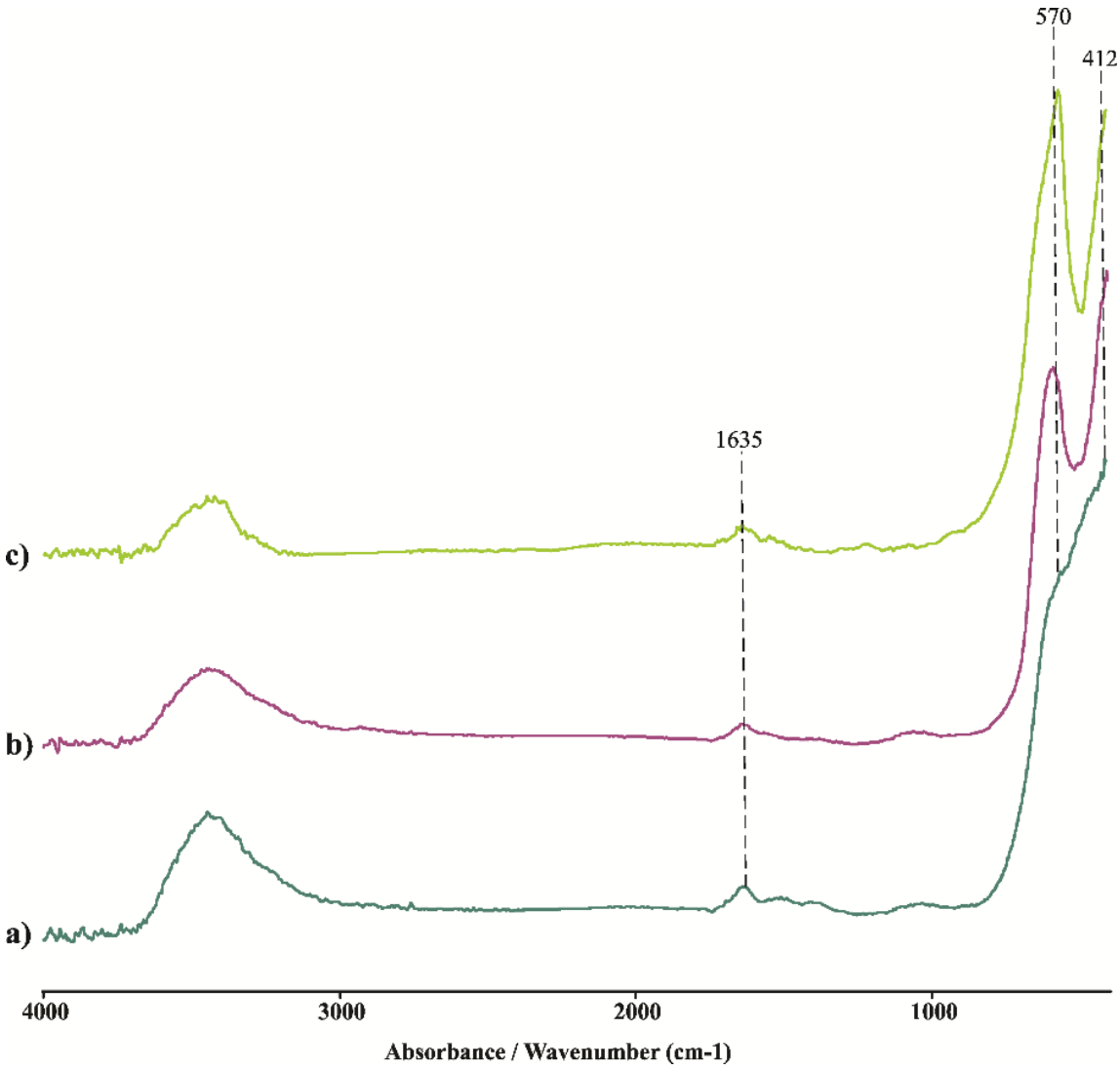

Fig. 4. FT-IR spectra of the powders calcined at different temperatures: a) 900 °C, b) 1200 °C, c) 1500 °C.

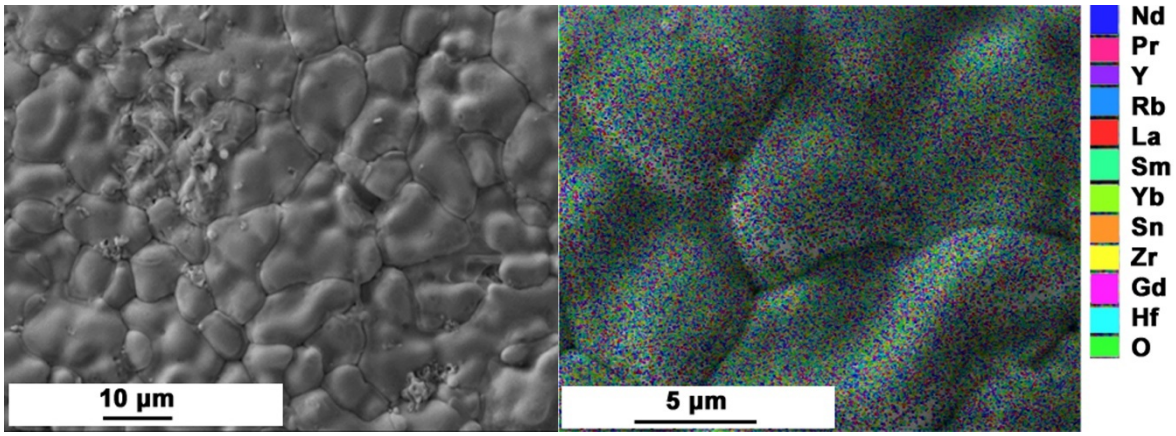

(a) (b)

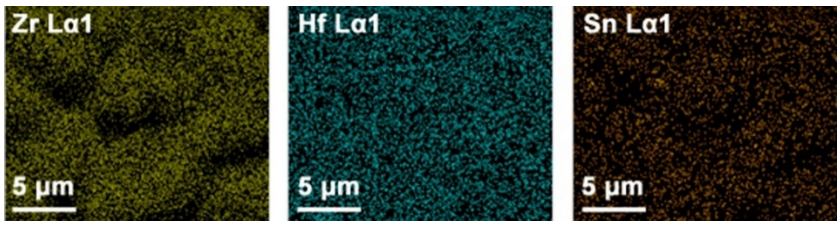

(c)

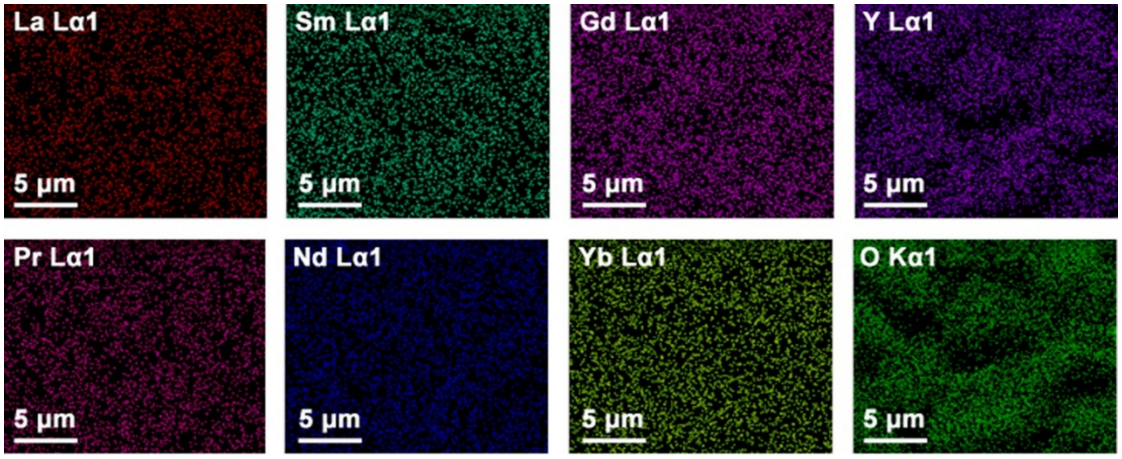

(d)

Fig. 5. a),c) SEM micrographs with c),d) corresponding EDS elemental maps of the pyrochlore compound $(La_{1/7}Sm_{1/7}Nd_{1/7}Pr_{1/7}Y_{1/7}Gd_{1/7}Yb_{1/7})_2(Sn_{1/3}Hf_{1/3}Zr_{1/3})_2O_7$ sintered at 1650 °C for 4 h showing a) grains morphology, b) grains contact, c) distribution of B-site elements, d) distribution of A-site elements and oxygen.

Tables

Tab. I Cell parameter, crystallite size, and lattice strain parameters of calcined $(La_{1/7}Sm_{1/7}Nd_{1/7}Pr_{1/7}Y_{1/7}Gd_{1/7}Yb_{1/7})_2(Sn_{1/3}Hf_{1/3}Zr_{1/3})_2O_7$ powders treated for 2 h at different temperatures. Structures are refined in space group 227.

Calcination temperature (°C)	900 °C	1200 °C	1500 °C
Lattice parameter *a* (Å)	10.5720(7)	10.5704(1)	10.5782(2)
Oxygen coordinate *x(O$_1$)*	0.3209(2)	0.3197(1)	0.33681(2)
Crystallite size (nm)	7.2(3)	65.7(6)	336.8(2)
Strain ($\times 10^{-3}$)	78.59(3)	50.03(2)	8.255(4)